Reduced Zirconium Halide Clusters in Aqueous Solution

Xiaobing Xie and Timothy Hughbanks*

Department of Chemistry, Texas A&M University, P.O. Box 30012 College Station, Texas 77842-3012

Received July 16, 1999

Reduced hexazirconium halide cluster compounds have good solubility and stability in strongly acidic and/or halide-rich aqueous solutions. Cyclic voltammetric (CV) measurements in aqueous media established that $[(Zr_6BCl_{12})(H_2O)_6]^{2+/+}$ and $[(Zr_6BBr_{12})(H_2O)_6]^{2+/+}$ exhibited positive half-wave potentials ($E_{1/2}$ = 0.059V and 0.160 V, respectively) vs the SHE, indicating that these clusters are only modestly reducing. Several new crystalline cluster compounds have been isolated from cold 12 M HCl solutions; the structures of each contain extended hydrogen-bonding water networks. Crystallographic data for these compounds are reported as follows: $[Rb_{0.44}(H_3O)_{4.56}][(Zr_6BCl_{12})Cl_6]\cdot 19.44H_2O$ (**3**), cubic, $Im\bar{3}m$, a = 13.8962(3) Å, Z = 2; $(H_3O)_5[(Zr_6BeCl_{12})Cl_6]\cdot 19H_2O$ (**4**), cubic, $Im\bar{3}m$, a = 13.8956(4) Å, Z = 2; $(H_3O)_5[(Zr_6MnCl_{12})Cl_6]\cdot 19H_2O$ (**5**), cubic, $Im\bar{3}m$, a = 14.029(3) Å, Z = 2; $(H_3O)_4[(Zr_6BCl_{12})Cl_6]\cdot 12.97H_2O$ (**6**), tetragonal, $P4_2/mnm$, a = 11.5373(2) Å, c = 15.7169(4) Å, Z = 2; $(H_3O)_4[(Zr_6BCl_{12})Br_6]\cdot 13.13H_2O$ (**7**), tetragonal, $P4_2/mnm$, a = 11.7288(6) Å, c = 15.931(1) Å, Z = 2.

Introduction

In standard compendia describing the reduced halides of zirconium, it is generally remarked that such compounds "are stable only in the solid phase, and react with water with evolution of hydrogen."[1] Indeed, experience with the reactivity of zirconium in lower oxidation states has prompted Soloveichik to generalize this characterization to all reduced compounds of zirconium and hafnium: "Low oxidation states are not characteristic of zirconium and hafnium. There is no aqueous chemistry of the metal in oxidation state = III."[2] Other texts contain similar summaries,[3,4] all of which were accurate until we recently discovered that some hexazirconium halide clusters are water-stable.[5]

The rich solid-state chemistry of centered hexazirconium halide clusters $[(Zr_6ZX_{12})X_6]^{m-}$ (Z = H, Be to N, Al to P, Mn to Ni; X = Cl, Br, I), in which reduced zirconium forms metal−metal bonds, was developed by Corbett and co-workers throughout the 1980s and early 1990s.[6−15] It had been generally assumed, and often observed, that these cluster compounds were as highly air- and moisture-sensitive as other reduced zirconium compounds. Indeed, in a preliminary investigation of the dissolution of these phases, (Zr_6ZX_{12})-based clusters were observed to "react with water, alcohol, and acetone, with both oxidation and solvolysis."[16]

The chemistry of centered hexazirconium halide clusters has been extended into solution via reactions in which clusters are excised from solid-state precursors.[17−21] Until recently, however, solvents for such reactions were limited to aprotic organic solvents with high dielectric constant (e.g., acetonitrile and sulfolane) and ionic liquids ($AlCl_3$/1-ethyl-3-methylimidazolium chloride, $AlCl_3$/ImCl). On the other hand, the structurally related niobium and tantalum halide cluster unit, $[M_6Cl_{12}]^{n+}$ (M = Nb, Ta; n = 2, 3, 4), are stable in deoxygenated water, and their aqueous chemistry has been explored.[22−28]

We recently found that some Zr_6ZCl_{12}-based clusters were sufficiently stable in methanol[29] or acidic and/or chloride-rich aqueous solutions to allow further investigation of their coordination chemistry. We have published a communication

(1) Eagleson, M. *Concise Encyclopedia of Chemistry*; Walter de Gruyter: Berlin, 1994.
(2) Soloveichik, G. L. In *Encyclopedia of Inorganic Chemistry*; King, R. B., Ed.; John Wiley & Son: Chichester, U.K., 1994; Vol. 8, pp 4475−4506.
(3) Cotton, F. A.; Wilkinson, G. *Advanced Inorganic Chemistry*, 5th ed.; John Wiley & Sons: New York, 1988.
(4) Greenwood, N. N.; Earnshaw, A. *Chemistry of the Elements*; Pergamon: New York, 1984.
(5) Xie, X.; Hughbanks, T. *Angew. Chem., Int. Ed.* **1999**, *38*, 1777−1779.
(6) Smith, J. D.; Corbett, J. D. *J. Am. Chem. Soc.* **1984**, *106*, 4618−4619.
(7) Ziebarth, R. P.; Corbett, J. D. *J. Am. Chem. Soc.* **1985**, *107*, 4571−4573.
(8) Smith, J. D.; Corbett, J. D. *J. Am. Chem. Soc.* **1985**, *107*, 5704−5711.
(9) Smith, J. D.; Corbett, J. D. *J. Am. Chem. Soc.* **1986**, *108*, 1927−1934.
(10) Ziebarth, R. P.; Corbett, J. D. *J. Am. Chem. Soc.* **1989**, *111*, 1, 3272−3280.
(11) Ziebarth, R. P.; Corbett, J. D. *Acc. Chem. Res.* **1989**, *22*, 256−262.
(12) Zhang, J.; Corbett, J. D. *Inorg. Chem.* **1991**, *30*, 431−435.
(13) Zhang, J. Ph.D. Dissertation, Iowa State University, 1990.
(14) Qi, R.-Y.; Corbett, J. D. *Inorg. Chem.* **1995**, *34*, 1657−1662.
(15) Qi, R.-Y.; Corbett, J. D. *Inorg. Chem.* **1995**, *34*, 1646−1651.
(16) Rogel, F.; Zhang, J.; Payne, M. W.; Corbett, J. D. In *Electron Transfer in Biology and the Solid State*; Johnson, M. K., King, R. B., Kurtz, D. M., Jr., Kutal, C., Norton, M. L., Scott, R. A., Eds.; American Chemical Society: Washington, DC, 1990; Vol. 226, pp 367−389.
(17) Rogel, F.; Corbett, J. D. *J. Am. Chem. Soc.* **1990**, *112*, 8198−8200.
(18) Rogel, F. Ph.D. Dissertation, Iowa State University, 1990.
(19) Tian, Y.; Hughbanks, T. *Inorg. Chem.* **1995**, *34*, 6250−6254.
(20) Runyan, C. E., Jr.; Hughbanks, T. *J. Am. Chem. Soc.* **1994**, *116*, 7909−7910.
(21) Runyan, C. E., Jr. Ph.D. Dissertation, Texas A&M University, 1994.
(22) Harned, H. S.; Pauling, C.; Corey, R. B. *J. Am. Chem. Soc.* **1960**, *82*, 4815−4817.
(23) Allen, R. J.; Sheldon, J. C. *Aust. J. Chem.* **1964**, *18*, 277−283.
(24) Fleming, P. B.; Dougherty, T. A.; McCarley, R. E. *J. Am. Chem. Soc.* **1967**, *89*, 159−160.
(25) Fleming, P. B.; Mueller, L. A.; McCarley, R. E. *Inorg. Chem.* **1967**, *6*, 1−4.
(26) Cooke, N. E.; Kuwana, T.; Espenson, J. *Inorg. Chem.* **1971**, *10*, 1081−1083.
(27) Brnicevic, N.; Planinic, R.; McCarley, R. E.; Antolic, S.; Luic, M.; Kojic-Prodic, B. *J. Chem. Soc., Dalton Trans.* **1995**, 1441−1446.
(28) Beck, U.; Simon, A.; Sirac, S.; Brnicevic, N. Z. *Anorg. Allg. Chem.* **1997**, *623*, 59−64.
(29) Xie, X.; Reibenspies, J. H.; Hughbanks, T. *J. Am. Chem. Soc.* **1998**, *120* 11391−11400.

10.1021/ic9908423 CCC: $19.00
Published on Web 01/21/2000

Table 1. Behavior of Centered Hexazirconium Clusters in Aqueous Media

precursor	solvent system	soln color	bleaching time
$Rb_5Zr_6Cl_{18}B$	H_2O	red	19 h
	4 M CF_3SO_3H		3 days
	12 M LiCl		weeks
	12 M HCl		weeks
$KZr_6Cl_{15}C$	H_2O	red	20 h
	12 M HCl		weeks
$Na_4Zr_6Cl_{16}Be$	H_2O	red	15 min
	12 M HCl		2 h
$KZr_6Cl_{15}Fe$	H_2O	colorless	immediate
	12 M HCl	blue	30 min
$Li_2Zr_6Cl_{15}Mn$	H_2O	colorless	immediate
	12 M HCl	green	30 min
$(K_4Br)_2Zr_6Br_{18}B$	H_2O	red	1 week
$(K_4Br)_2Zr_6Br_{18}Be$	H_2O	red	5 h

describing the behavior hexazirconium chloride clusters in aqueous solutions and the isolation of $(H_3O)_5[(Zr_6BCl_{12})Cl_6]\cdot 19H_2O$ (**1**) and $(H_3O)_4[(Zr_6CCl_{12})Cl_6]\cdot 12.93H_2O$ (**2**).[5] In this paper, we report electrochemical measurements on $[Zr_6ZX_{12}]^{n+}$ (Z = Be, B, C; X = Cl, Br) clusters in various aqueous solutions and the isolation of several hexazirconium cluster compounds, $[Rb_{0.44}(H_3O)_{4.56}][(Zr_6BCl_{12})Cl_6]\cdot 19.44H_2O$ (**3**), $(H_3O)_5[(Zr_6BeCl_{12})Cl_6]\cdot 19H_2O$ (**4**), $(H_3O)_5[(Zr_6MnCl_{12})Cl_6]\cdot 19H_2O$ (**5**), $(H_3O)_4[(Zr_6BCl_{12})Cl_6]\cdot 12.97H_2O$ (**6**), and $(H_3O)_4[(Zr_6BCl_{12})Br_6]\cdot 13.13H_2O$ (**7**), from strongly acidic solutions.

Experimental Section

Techniques and Materials. All compounds were manipulated in a nitrogen atmosphere glovebox or in Schlenk (Ar) or high-vacuum lines. The solid-state cluster precursors, $Rb_5Zr_6Cl_{18}B$, $Na_4Zr_6Cl_{16}Be$, $Rb_4Zr_6Cl_{18}C$, $Li_2Zr_6Cl_{15}Mn$, $LiZr_6Cl_{15}Fe$, $(K_4Br)_2Zr_6Br_{18}B$, and $(K_4Br)_2Zr_6Br_{18}Be$, were synthesized by use of published procedures.[7,10,12,30,31] Syntheses of these cluster precursors were confirmed by Guinier X-ray powder diffraction. All metal halides were sublimed under vacuum prior to use. Zr powder is prepared from Zr foil by a hydrogenation−dehydrogenation process that has been described previously.[8] Boron (Alfa), beryllium (Aldrich), and ^{13}C (Isotec. Inc.) powders were used as received. Water, hydrochloric acid (38%, EM), and hydrobromic acid (48%, Fisher) were all deoxygenated in three freeze−thaw cycles on a vacuum line prior to their storage in a nitrogen-purged box. Trifluoromethanesulfonic acid (Aldrich) was diluted with deoxygenated water to ~4 M concentration and stored in a nitrogen-purged box.

Dissolution of the Cluster Precursors. In each case, a solid precursor (30−40 mg) was loaded in an ampule, to which solvent (water or acidic solution) was added by use of a syringe. The mixture was shaken for a few minutes, and insoluble solids (usually a trace amount) were separated by centrifugation. A syringe was then used to decant the colored supernatant. In some cases, the solution bleached over time and bubbles were observed; detailed observations concerning particular cases are summarized in Table 1.

NMR. ^{11}B solution NMR spectra were measured on a Varian XL 200 broad-band spectrometer (at 64.18 MHz). Typically, 2.5 mL of a solution containing B-centered cluster species was transferred to a 10-mm NMR tube, and a coaxial inner tube with deuterated benzene (C_6D_6) or acetone (CD_3COCD_3) was inserted. Chemical shifts for ^{11}B are reported with respect to the external standard $BF_3\cdot OEt_2$ ($\delta = 0$). Acquisition times of 2 s were usually used; 1000−5000 transients were usually required to obtain reasonably good signal-to-noise ratios. In two recently published papers, we have described the use of multinuclear NMR spectroscopy for monitoring cluster speciation in solution, especially those centered by boron.[29,32] Detailed explanations of our peak assignments are not given here.

Electrochemical Studies. For a set of measurements, the solution to be studied was transferred into an 8-mL five-neck flask. Each neck was covered by a septum; three of the necks are used to pass through electrodes, and when necessary, two necks allow for purging with inert gas. CV experiments were carried out with a BAS 100B/W electrochemical workstation (Bioanalytical Systems, West Lafayette, IN). A glassy carbon disk electrode served as a working electrode, the counter electrode was platinum wire, and the reference electrode was AgCl/Ag in 3 M aqueous NaCl solution.

X-ray Structure Determinations. In each case, 10−15 mg of a solid cluster precursor was combined with 1.0 mL of deoxygenated 12 M HCl (for **3**−**6**) or 6 M HBr (for **7**) in an ampule and shaken for about 1 min. After centrifugation, the colored solution was transferred into a long glass tube that was sealed on a Schlenk line and put into a freezer (−20 °C) for 3 days, whereupon deeply colored crystals were invariably observed below a colorless supernatant. Single-crystal structure determinations were undertaken for five cluster complexes (**3**−**7**).

In each case, immediately upon its removal from the mother solution, a crystal was coated with Apiezon-T stopcock grease, mounted on the tip of a glass fiber, and then inserted into the low-temperature nitrogen stream of the diffractometer for data collection. Data were collected at −60 °C using a Siemens (Bruker) SMART CCD (charge-coupled device) equipped diffractometer with an LT-2 low-temperature apparatus. For all crystals, a hemisphere of data was collected using ω scans of 0.3° per frame for 30 s. A total of 1271 frames were collected with a maximum resolution of 0.75 Å. The first 50 frames were recollected at the end of data collection to check for decay. Cell parameters were retrieved using SMART software[33] and refined using SAINT software[34] on all observed reflections. Data reduction was performed using SAINT, which corrects for Lorentz polarization and decay. Multiscan absorption correction and secondary extinction corrections were applied. Initial zirconium positions were obtained from the SHELXS-93 direct method output. Subsequently, the other non-hydrogen atomic positions were located directly from the electron density difference maps. Structural refinement was performed on F^2 by the least-squares method using the SHELXL-97 package,[35] incorporated in SHELXTL-PC V5.03.[36] Thermal parameters for all non-hydrogen atoms in the unit cell were refined anisotropically. Although hydrogen atoms could often be located in subsequent difference Fourier syntheses, none were included in final structural refinements. Pertinent crystallographic data for all compounds are summarized in Table 2.

For **3**−**5**, the cubic space group $Im\bar{3}m$ was chosen on the basis of intensity statistics and the observed systematic absences. In the structural refinement of the crystal of **3**, a residual electron density peak (4.75 e/Å^3) appeared at the D_{3d} ($^1/_4$, $^1/_4$, $^1/_4$) symmetry site after anisotropic refinement of all Zr, Cl, and O atoms. This site locates in the center of each puckered hexagon formed by six oxygen atoms. At this stage of the refinement, $R_1 = 5.00\%$ and $wR^2 = 21.77\%$. Further refinements yielded 11% Rb atom (or 50% O atom) occupancy at this site with the R_1 and wR^2 respectively dropping to 2.77% (2.78%) and 10.04% (10.15%). The simultaneous refinement of thermal parameter and occupancy at this site favors the rubidium case. Thus, in the final cycle of the refinement this site was assumed to occupied solely by Rb, for which both occupancy and anisotropic parameters were refined. This yielded the composition $[Rb_{0.44}(H_3O)_{4.56}][(Zr_6BCl_{12})Cl_6]\cdot 19.44H_2O$ for this crystal. As discussed below, mixed Rb^+/H_3O^+ occupancy of this D_{3d} symmetry site might best represent reality.

For the structures of **6** and **7**, the tetragonal $P4_2/mnm$ space group was chosen on the basis of intensity statistics and the observed

(30) Zhang, J.; Ziebarth, R. P.; Corbett, J. D. *Inorg. Chem.* **1992**, *31*, 614−619.
(31) Qi, R.-Y.; Corbett, J. D. *Inorg. Chem.* **1997**, *36*, 6039−6044.
(32) Harris, J. D.; Hughbanks, T. *J. Am. Chem. Soc.* **1997**, *119*, 9449−9459.
(33) SMART V 4.043: *Software for the CCD Detector System*; Bruker Analytical X-ray System: Madison, WI, 1995.
(34) SAINT V 4.035: *Software for the CCD Detector System*; Bruker Analytical X-ray System: Madison, Madison, WI, 1995.
(35) SHELXL-97: Sheldrick, G. M. *Program for the Refinement of Crystal Structure*: University of Göttingen: Göttingen, Germany, 1997.
(36) SHELXTL 5.10 (PC-version): *Program library for Structure Solution and Molecular Graphics*; Bruker Analytical X-ray Systems: Madison, WI, 1998.

Table 2. Crystallographic Data for Centered Zirconium Halide Cluster Compounds Isolated from Acidic Aqueous Solutions

	3	**4**	**5**	**6**	**7**
chem formula	$H_{52.56}BCl_{18}O_{24}Rb_{0.44}Zr_6$	$H_{53}BeCl_{18}O_{24}Zr_6$	$H_{53}MnCl_{18}O_{24}Zr_6$	$H_{37.93}BCl_{18}O_{16.97}Zr_6$	$H_{38.26}BBr_6Cl_{12}O_{17.13}Zr_6$
fw	1670.76	1631.85	1677.78	1510.59	1773.29
space group	$Im\bar{3}m$	$Im\bar{3}m$	$Im\bar{3}m$	$P4_2/mnm$	$P4_2/mnm$
a, Å	13.8962(3)	13.8956(4)	14.029(3)	11.5375(2)	11.7288(6)
c, Å				15.7169(4)	15.931(1)
V, Å^3	2683.4(1)	2683.1(1)	2761(1)	2092.14(7)	2191.5(2)
Z	2	2	2	2	2
ρ_{calcd}, g cm^{-3}	2.068	2.020	2.018	2.398	2.687
μ, mm^{-1}	2.472	2.075	2.235	2.640	7.624
radiation, Å (Mo)	0.710 73	0.710 73	0.710 73	0.710 73	0.710 73
T, °C	−60.0	−60.0	−60.0	−60.0	−60.0
$R_1{}^a$ ($I > 2\sigma(I)$)	0.0264	0.0245	0.0278	0.0259	0.0241
wR^2 [b]	0.0646	0.0687	0.0692	0.0574	0.0581

[a] $R_1 = \sum||F_o| - |F_c||/\sum|F_o|$. [b] $wR^2 = [\sum[w(F_o^2 - F_o^2)^2]/\sum[w(F_o^2)^2]]^{0.5}$.

systematic absences. These two compounds have virtually the same structure as **2**.[5] The diffraction data for **2** exhibit what superficially appears to be a tetragonal $\sqrt{2} \times \sqrt{2} \times 2$ superlattice but is likely the result of a subtle twinning of a lower symmetry superlattice that we have not yet determined. On one site, which is surrounded by four water molecules that form a tetrahedron at a distance to oxygen of ~2.85 Å, partial occupancy by water was indicated for both crystals. The electron density residues there (~3.5 e/Å^3) were modeled by assuming partial oxygen atom occupancy (O4) and refined at 48% and 57% for **6** and **7**, respectively.

Results and Discussion

Dissolution of the $[Zr_6ZX_{12}]^{n+}$ Clusters in Aqueous Media. Each of the solid-state cluster precursors we have chosen readily dissolve, and their solutions exhibit characteristic colors: main-group-centered clusters are red, $[Zr_6FeX_{12}]^{2+}$ solutions are deep blue, and $[Zr_6MnX_{12}]^{+}$ solutions are dark green. The rates at which color is bleached reflect rates of cluster decomposition (sometimes not at all, sometimes with observable generation of hydrogen bubbles). In pure water at ambient temperature, solutions of Fe- and Mn-centered clusters decolorize immediately upon dissolution, and a solution of the Be-centered cluster bleaches within 20 min. In contrast, the red aqueous solutions obtained by dissolving hexazirconium clusters with smaller interstitial atoms (B or C) in water bleach much more slowly. It is also notable that $[Zr_6ZBr_{12}]^{n+}$ (Z = B, Be) clusters survive longer in water than their chloride analogues. Not surprisingly, cooling the solutions slows cluster decomposition.

Most Zr_6ZX_{12}-based cluster compounds decompose fairly quickly in water, as observed by other workers.[16] However, we find that $[Zr_6ZX_{12}]^{n+}$ cluster species exhibit dramatically improved stability in strongly acidic and/or halide-rich aqueous solution (Table 1). A solution formed by dissolving $Rb_5Zr_6Cl_{18}B$ in 4 M CF_3SO_3H bleaches only slowly (3 days) at room temperature, while the solutions formed by dissolving $Rb_5Zr_6Cl_{18}B$ in 12 M HCl or 12 M LiCl retain their characteristic red color indefinitely at room temperature. In contrast, immediate cluster decomposition was evidenced by vigorous bubbling and rapid loss of the red color when $Rb_5Zr_6Cl_{18}B$ was dissolved in a dilute aqueous NaOH solution.

Although we offer no detailed mechanism of cluster decomposition in aqueous solution, our qualitative observations suggest that the first steps of cluster decomposition involve the formation of clusters with terminal hydroxide ligands, $[(Zr_6Cl_{12}B)(H_2O)_{6-x}(OH)_x]^{1-x}$. We measured the pH of a freshly prepared 4.6×10^{-3} M aqueous solution of $Rb_5Zr_6Cl_{18}B$ to be 3.4, suggesting that the principal observable cluster species, $[(Zr_6BCl_{12})(H_2O)_6]^+$, acts as a weak Brønsted acid ($pK_a \approx 4.4$) via deprotonation of ligated water:

$$[(Zr_6BCl_{12})(H_2O)_6]^+ \rightleftharpoons H^+(aq) + [(Zr_6BCl_{12})(H_2O)_5(OH)]$$

Here it is understood that deprotonation of additional bound water ligands may also occur. Over time, this solution becomes more acidic as the cluster slowly decomposes. Clearly, this deprotonation should be extensively suppressed in strongly acidic solutions. In the presence of excess chloride ions, the formation of clusters with terminal hydroxide should become unfavorable because of the chlorides' competition for terminal binding sites (as evidenced by ^{11}B NMR spectra)[5] and because the Brønsted acidity of $[(Zr_6BCl_{12})Cl_x(H_2O)_{6-x}]^{1-x}$ anions is presumably lower than the cationic hexaaquo cluster.

Since several of the hexazirconium chloride clusters are stabilized in acidic aqueous solutions, we were able to isolate a number of crystalline hexazirconium halide cluster compounds (**1**−**7**) by dissolving the solid-state precursors in concentrated HX (X = Cl and Br) acids at ambient temperature and then recrystallizing at −20 °C. Clusters with interstitial B and C atoms are quite stable in aqueous HX solutions, and they (**1**−**3**) can be isolated in yields of up to 70% by this process. In contrast, clusters with larger interstitial atoms (Be, Mn, and Fe) decompose relatively quickly in 12 M HCl solution. **4** and **5** were therefore recovered in low yields, and no single crystals containing Fe-centered clusters were obtained. Even in crystalline form, **5** decomposes in about 2 weeks at −20 °C.

Crystal Structures. Compounds isolated from cold hydrohalic acids that contain $[(Zr_6ZCl_{12})X_6]^{m-}$ (X = Cl or Br; m = 4, 5) clusters are segregated into two types as far as their structures are concerned. Compounds containing clusters with a charge of 5−, $[(Zr_6ZCl_{12})Cl_6]^{5-}$ (Z = Be, B, Mn), adopt isotypic cubic structures, while those with clusters bearing a 4− charge, $[(Zr_6ZCl_{12})X_6]^{4-}$ (Z = C, B; X = Cl or Br), adopt isotypic tetragonal structures.

(a) Cubic Structure. 3−**5**, which are isotypic with the previously reported **1**,[5] crystallize in the cubic $Im\bar{3}m$ space group. The $[(Zr_6ZCl_{12})Cl_6]^{5-}$ (Z = B, Be, Mn) clusters exhibit perfect O_h symmetry with their Z atoms on the origin (and center) of the unit cell. These clusters are surrounded by intriguing water cages that are held together by the hydrogen bonds among water molecules and hydronium ions. These water cages link with the terminal chloride ligands of the clusters via weak Cl^a···H−O interactions as shown in Figure 1.

When $Rb_5Zr_6Cl_{18}B$ is used as the precursor instead of $Na_2Zr_6Cl_{15}B$, the cluster compounds obtained apparently contain a

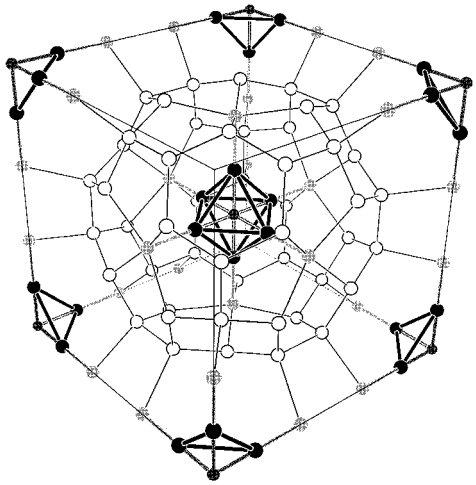

Figure 1. Unit cell packing diagram for **3** (isotypic with **4** and **5**). Black circles represent zirconium atoms, open circles are oxygen atoms of water molecules, and shaded circles are the terminal chlorides of the clusters. Two cluster fragments at the corners of the cube (foreground and background) and the inner bridging chlorides (Cl^i) have been omitted.

Table 3. Selected Bond Lengths (Å) and Angles (deg) for **1** and **3**−**5**

	$[(Zr_6ZCl_{12})Cl_6]^{5-}$			
	Z = B (**1**)	Z = B (**3**)	Z = Be (**4**)	Z = Mn (**5**)
Zr−Z	2.2994(5)	2.3042(7)	2.3585(8)	2.4140(9)
Zr− Zr	3.2519(8)	3.259(1)	3.335(1)	3.414(1)
Zr−Cl^i	2.5512(8)	2.557(1)	2.561(1)	2.583(1)
Zr−Cl^a	2.661(2)	2.657(2)	2.646(2)	2.677(2)
trans-Cl−Zr−Cl	169.18(4)	169.19(5)	171.25(6)	172.74(6)
water network				
O···O	2.743(4)	2.765(4)	2.806(8)	2.751(6)
O···O	2.810(7)	2.790(7)	2.747(4)	2.87(1)
O···Cl^a	3.200(3)	3.196(4)	3.202(4)	3.236(5)

small amount of rubidium and differ from **1** only in that respect. Atomic absorption analyses on bulk samples confirm the presence of rubidium but indicate only about half as much Rb as we obtain from crystallographic refinement when we assume the electron density peak at ($^1/_4$, $^1/_4$, $^1/_4$) is entirely due to rubidium. Of course, it is quite conceivable that the rubidium content of the crystal we selected for X-ray data collection is greater than is present in the bulk sample. Both Rb^+ and H_3O^+ ions have been observed in similar environments within the macrocyclic 18-crown-6 polyether.[37−39] The Rb−O distances of ∼2.90 Å observed in crown ether complexes were considerably longer than the distance of 2.732(4) Å between the center of the hexagon and the six surrounding oxygen atoms in **3**, but some local expansion of the oxygen coordination shell could occur in sites that are actually occupied; i.e., the observed distance of 2.732(4) Å may merely represent a weighted average over occupied and vacant sites.

Selected bond distances and bond angles associated with clusters in **1** and **3**−**5** are listed in Table 3. The Zr−Be and Zr−Zr distances (2.3585(8) and 3.335(1) Å, respectively) in **4** are significantly longer than typical corresponding distances (2.333 and 3.300 Å) for compounds containing Be-centered clusters with 14 CBEs (cluster-based electrons).[17,40,41] This is consistent with our formulation of **4** as a 13 CBE cluster compound as the result of one-electron oxidation of the clusters in the solid precursor. Electrochemical data (discussed below) demonstrate that Be-centered cluster with 14 CBEs is thermodynamically unstable with respect to one-electron oxidation by protons in strong aqueous acids.

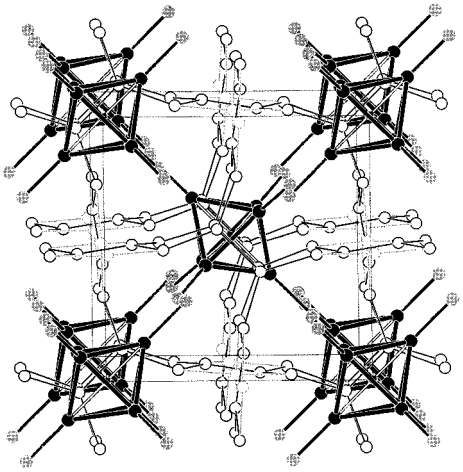

Figure 2. Unit cell packing diagram for **6** (isotypic with **7**). Black circles represent zirconium atoms, the open circles are oxygen atoms of water molecules, and shaded circles are the terminal chlorides of the clusters. The inner bridging chlorides (Cl^i) have been omitted.

A comparison of information in Table 3 with that in previously published reports[10,12,42] clearly demonstrates that the structural features and trends exhibited by $[(Zr_6ZCl_{12})Cl_6]^{5-}$ clusters we have isolated are substantially the same as in appropriate solid-state precursors, as one would expect. Clusters with larger interstitial atoms have longer Zr−Z and Zr−Zr distances, and Zr−Cl^i distances change little when the Zr_6Z cluster core expands to accommodate larger interstitial atoms. As a consequence, *trans*-Cl^i−Zr−Cl^i angles increase and steric crowding at the terminal position should decrease as the interstitial atom size increases. It follows that access of nucleophiles to the $[Zr_6ZCl_{12}]^{n+}$ cluster core should increase as interstitial atom size increases on moving along the series C < B < Be < Mn. This structural correlation is in correspondence with the generally greater stability we observe for C- and B-centered clusters in water and in the presence of other nucleophiles. A more pronounced "matrix effect"[43] should apply to bromide-supported clusters, $[Zr_6ZBr_{12}]^{n+}$, where steric congestion is even greater (*trans*-Br^i−Zr−Br^i angles are 165° in $[Zr_6BBr_{12}]^+$).[44] This steric congestion is probably the principal factor responsible for the extended 'lifetimes' of bromide-supported clusters in comparison with their chloride analogues under the same conditions in aqueous solution.

(b) Tetragonal Structure. Both **6** and **7** crystallize in the tetragonal space group $P4_2/mnm$; a projection of the structure shown in Figure 2. Since the B-centered clusters have 13 CBEs in both cases, the formation of these two compounds was either the result of adventitious oxidation of the cluster precursor by impurities (probably O_2) or oxidation by protons in a reaction that was accelerated by trace catalytic impurities in the solvent

(37) Atwood, J. L.; Bott, S. G.; Coleman, A. W.; Robinson, K. D.; Whetstone, S. B.; Means, C. M. *J. Am. Chem. Soc.* **1987**, *109*, 8100−8101.
(38) Rogers, R. D.; Bond, A. H.; Hipple, W. G.; Rollins, A. N.; Henry, R. F. *Inorg. Chem.* **1991**, *30*, 2671−2679.
(39) Truter, M. R. *Struct. Bonding* **1973**, *16*, 71−111.
(40) Ziebarth, R. P.; Corbett, J. D. *Inorg. Chem.* **1989**, *28*, 626−631.
(41) Ziebarth, R. P.; Corbett, J. D. *J. Am. Chem. Soc.* **1988**, *110*, 1132−1139.
(42) Tian, Y.; Hughbanks, T. *Z. Anorg. Allg. Chem.* **1996**, *622*, 425−431.
(43) Corbett, J. D. *Acc. Chem. Res.* **1981**, *14*, 239−246.
(44) Xie, X.; Hughbanks, T. *Solid State Sci.* **1999**, *1*, 463−472.

Table 4. Selected Bond Lengths (Å) and Angles (deg) for **2**, **6**, and **7**

	$[(Zr_6ZCl_{12})X_6]^{4-}$		
	Z = C, X = Cl (**2**)	Z = B, X = Cl (**6**)	Z = B, X = Br (**7**)
$Zr_{ax}-Z$	2.3045(5) × 2	2.3536(8) × 2	2.3448(9) × 2
$Zr_{eq}-Z$	2.2825(3) × 4	2.3291(5) × 4	2.3245(7) × 4
$Zr_{eq}-Zr_{ax}$	3.2435(8) × 8	3.3112(6) × 8	3.3017(8) × 8
$Zr_{eq}-Zr_{eq}$	3.2192(7) × 2	3.271(1) × 2	3.271(1) × 2
	3.2365(7) × 2	3.317(1) × 2	3.304(1) × 2
$Zr_{ax}-X^a$	2.598(1)	2.579(2)	2.743(1)
$Zr_{eq}-X^a$	2.6426(8)	2.631(2)	2.787(1)
$Zr-Cl^i$	2.5352(7)	2.542(1)	2.541(2)
trans-Cl−Zr−Cl	169.38(3)	171.07(5)	170.90(6)

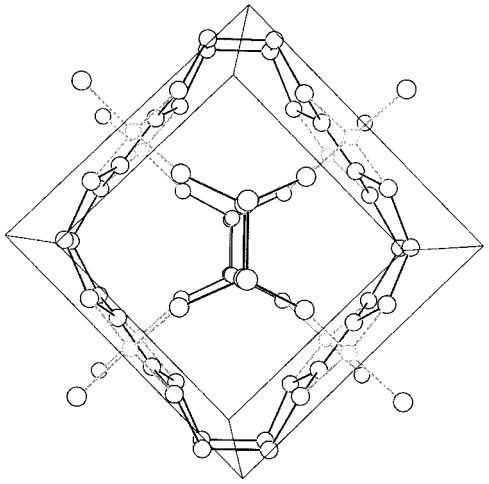

Figure 3. The water network that surrounds the $[(Zr_6ZCl_{12})X_6]^{4-}$ cluster units in **6** and **7**, viewed down the *c*-axis.

(see below). Selected bond distances and bond angles associated with the cluster compounds are listed in Table 4. Average Zr−B, Zr−Zr, and $Zr-Cl^i$ distances observed in **6** and **7** are all within the ranges expected, based on corresponding distances seen previously reported B-centered hexanuclear zirconium clusters with 13 CBEs.[17,42] The Zr_6 octahedra in **2**, **6**, and **7** are slightly asymmetric; in Table 4 this is manifest most noticeably in the relative shortening of two Zr−Zr bonds and in the fact that one Zr−Zr axis is longer than the other two. The source of the asymmetry in **2** probably arises from differences in hydrogen-bonding interactions between $Cl^{i/a}$ and the lattice water molecules surrounding the clusters. However, the more marked asymmetry in the open-shell 13 CBE B-centered clusters (**6** and **7**) may reflect an additional electronic effect, since these otherwise octahedral clusters would have $(t_{2g})^5$ configurations.[45,46]

The water network present in **2**, **6**, and **7** (Figure 3) differs substantially from that seen in **1** and **3**−**5**. The short O···O contacts connect the lattice water molecules and hydronium ions to form waved ribbons that wrap around the $[(Zr_6ZCl_{12})X_6]^{4-}$ clusters. These O···O distances range from 2.41 to 2.85 Å—well in the range of hydrogen-bonding interactions. The ribbons are interconnected by O(2)···O(2) contacts and contacts to a partially occupied (∼50%) water molecule on one site, about which the oxygen atoms of four water molecules in two neighboring ribbons are tetrahedrally situated at a distance of ∼2.85 Å. The presence of additional (acidic) protons can be inferred from the existence of short O···O contacts: the two shortest O···O distances, 2.425(6) and 2.53(1) Å, are close to those observed in $(H_5O_2)^+$ ions.[47] There are 4 such contacts per cluster so that charge balance is achieved by inclusion of $(H_5O_2)^+$ ions as the sole countercations.

Electrochemical Studies. As we stated in the Introduction, it was generally assumed that hexazirconium clusters would reduce protons in aqueous solution to hydrogen. However, we have seen that several zirconium clusters are quite stable in aqueous solution, and a few cluster species (either unoxidized or oxidized) have been isolated from their aqueous solutions. To more clearly assess the reducing strength of hexazirconium halide clusters, we have performed CV measurements on these cluster compounds in both 4 M triflic acid (CF_3SO_3H) and 12 M hydrochloric acid (HCl). The results are summarized in Table 5. The reader may wish to compare data reported here with those in our recent electrochemical investigation of hexazirconium clusters in chloroaluminate ionic liquids.[48] In that study, we demonstrated that Be-, B-, and C-centered hexazirconium clusters exhibit multiple waves corresponding to 11/12, 12/13, and 13/14 CBE redox couples and showed the systematic way in which redox potentials for these couples could be interrelated.

(a) $[Zr_6ZCl_{12}]^{n+}$ (Z = Be, B, C) in 4 M CF_3SO_3H. $Na_4Zr_6Cl_{16}Be$, $Rb_5Zr_6Cl_{18}B$, and $KZr_6Cl_{15}C$ can be readily dissolved in 4 M CF_3SO_3H to yield orange-red solutions. The ^{11}B NMR spectrum of the solution containing B-centered clusters consists of a lone singlet at δ = 189.9 ppm, indicating the exclusive presence of the hexaaquo species, $[(Zr_6BCl_{12})(H_2O)_6]^+$.[5] A cyclic voltammogram recorded for this solution is shown in Figure 4a. Upon scanning of the potential in the positive direction from the rest potential (−0.237 V), a one-electron oxidation wave that we attribute to the $[(Zr_6BCl_{12})(H_2O)_6]^{2+/+}$ redox couple was observed at $E_{1/2}$ = 0.060 V (vs SHE). The peak potential separation (ΔE_p) is 0.061 V, as expected for a diffusion controlled redox electrode reaction. The peak ratio (i_p^c/i_p^a) is 0.79, probably indicating that the oxidation product, $[(Zr_6BCl_{12})(H_2O)_6]^{2+}$, is only marginally stable on the time scale of the scan. The large irreversible wave observed at more positive potential (0.528 V) is undoubtedly a multielectron process associated with cluster decomposition and formation of Zr^{IV} species.

Unfortunately, triflic acid solutions containing Be-centered clusters quickly bleach (∼30 min) and $[(Zr_6BeCl_{12})(H_2O)_6]$ species do not survive long enough at room temperature to give useful electrochemical data. A similar solution of the C-centered hexaaquo ion, $[(Zr_6CCl_{12})(H_2O)_6]^{2+}$, is adequately stable, but no well-defined redox couples are observed by cyclic voltammetry. A large irreversible wave corresponding to cluster decomposition is observed at 0.381 V.

(b) $[Zr_6ZBr_{12}]^{n+}$ (Z = Be, B) in 4 M CF_3SO_3H. $(K_4Br)_2Zr_6Br_{18}B$ dissolves readily in 4 M triflic acid to form a dark red solution. $(K_4Br)_2Zr_6Br_{18}B$ is an unusual 15 CBE cluster precursor,[31] but when it is dissolved in aqueous solution, the presence of a single sharp resonance at δ = 199 ppm clearly indicates that the diamagnetic (14 CBE) cation, $[(Zr_6BBr_{12})(H_2O)_6]^+$, is the predominant species in solution. We presume that the observed one-electron cluster oxidation has occurred by reduction of protons.[44] The cyclic voltammogram for this solution exhibits a redox wave which is very similar to that observed for the chloride analog: the 13/14 CBE couple gives rise to a

(45) Hughbanks, T. *Prog. Solid State Chem.* **1989**, *19*, 329−372.
(46) Hughbanks, T.; Rosenthal, G.; Corbett, J. D. *J. Am. Chem. Soc.* **1988**, *110*, 1511−1516.
(47) Lundgren, J.-O.; Olovsson, I. *The Hydrated Proton in Solids*; Schuster, P., Zundel, G., Sandorfy, C., Eds.; North-Holland: Amsterdam, 1976; Vol. II, pp 473−523.
(48) Sun, D.; Hughbanks, T. *Inorg. Chem.* **1999**, *38*, 992−997.

Table 5. Summary of Electrochemical Data for Centered Zirconium Halide Clusters in Acidic Aqueous Solutions

	13/14 CBEs			12/13 CBEs		
solution	$E_{1/2}$, V	ΔE_p, V	i_p^c/i_p^a	$E_{1/2}$, V	ΔE_p, V	i_p^c/i_p^a
$Rb_5Zr_6Cl_{18}B$ in 4 M CF_3SO_3H	0.060	0.061	0.79		NA	
$(K_4Br)_2Zr_6Br_{18}B$ in 4 M CF_3SO_3H	0.159	0.067	0.87		NA	
$(K_4Br)_2Zr_6Br_{18}Be$ in 4 M CF_3SO_3H	−0.391	0.105	0.99	0.022	0.097	0.38
$Na_4Zr_6Cl_{16}Be$ in 12 M HCl	−0.662	0.083	0.14[a]	−0.275	0.082	0.69
$Rb_5Zr_6Cl_{18}B$ in 12 M HCl	−0.028	0.101	0.90		NA	

[a] This is a reduction wave; the value of i_p^a/i_p^c is given.

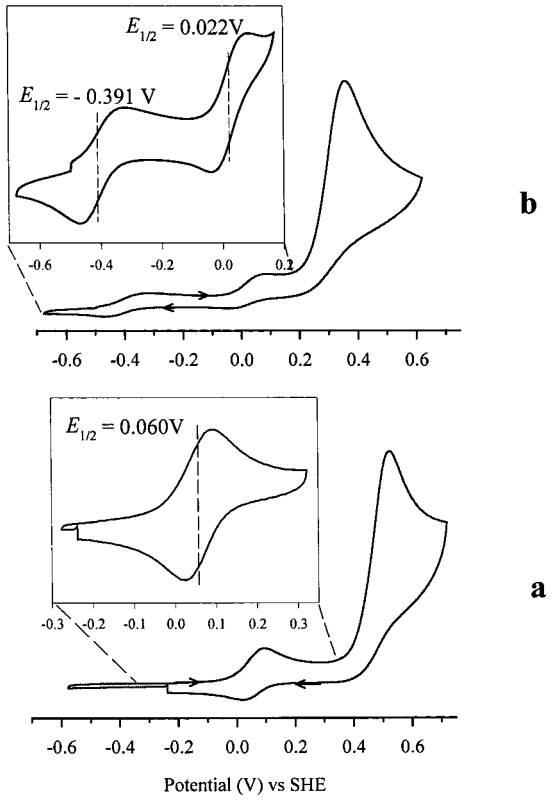

Figure 4. (a) Cyclic voltammogram for a 5×10^{-3} M solution of $Rb_5Zr_6Cl_{18}B$ in 4 M triflic acid. (b) Cyclic voltammogram for a 5×10^{-3} M solution of $(K_4Br)_2Zr_6Br_{18}Be$ in 4 M triflic acid.

well-defined redox wave centered at $E_{1/2} = 0.159$ V (vs SHE) and a large irreversible oxidative wave at 0.606 V that corresponds to cluster decomposition and formation of Zr^{IV} species. The separation of the peak potential (ΔE_p) for the redox wave is 0.067 V, indicating that the electrode reaction is nearly reversible. The ratio of peak current (i_p^c/i_p^a) is 0.87, suggesting that the species generated by oxidation is again not stable on the time scale of cyclic voltammetry (3000 mV/s). Despite the fact that clusters in the solid-state precursor possess 15 CBEs, no reduction wave corresponding to a 14/15 CBE couple is observed. This reduction presumably would be found at a potential outside the electrochemical window (more negative than −1.1 V, which is the apparent overpotential for proton reduction on the glassy carbon electrode).

$(K_4Br)_2Zr_6Br_{18}Be$ can be readily dissolved in 4 M triflic acid to form a dark red solution. This red solution is more stable than a solution of corresponding chloride cluster, and its cyclic voltammogram (Figure 4b) exhibits two distinct redox waves centered at −0.391 and 0.022 V, respectively corresponding to 13/14 CBE and 12/13 CBE redox couples. The familiar irreversible multielectron wave that signals oxidative cluster decomposition is observed at 0.362 V. The rest potential of the solution is −0.453 V, consistent with the 14 CBE oxidation state of the cluster found in the solid precursor. The peak current ratios (i_p^c/i_p^a) are 0.99 and 0.38 for 13/14 and 12/13 couples, respectively, indicating that, on the CV time scale, clusters with 13 CBEs are stable while those with 12 CBEs are not. The peak separations ($\Delta E_p \approx 0.100$ V) for both redox couples are larger than 0.060 V expected for a diffusion controlled redox electrode reactions.

(c) $[Zr_6ZCl_{12}]^{n+}$ (Z = Be, B, C) in 12 M HCl. In 12 M HCl, competition between chloride ions and water for terminal binding sites is clearly important, as indicated by the ^{11}B NMR studies of B-centered cluster in the aqueous solutions. The ^{11}B NMR spectrum of the solution obtained by dissolution of $Rb_5Zr_6Cl_{18}B$ in 12 M HCl shows a broad (∼100 Hz) peak centered near 186 ppm. The breadth of this peak arises from Cl^-/H_2O-exchange among the cluster species, $[(Zr_6BCl_{12})Cl_x(H_2O)_{6-x}]^{1-x}$ ($x = 0-6$), on the NMR time scale. In 12 M LiCl solution, the exchange rate among these species is slow enough at 25 °C that resonances for cluster complexes with different numbers of chloride ligands can be easily resolved and are separated by 35−45 Hz. (Resonances for geometric isomers cannot be resolved in aqueous solution,[5] but are quite evident in MeCN or MeOH).[29] The coalescence of these resonances in 12 M HCl therefore implies that lifetimes of individual species are $\lesssim 10^{-2}$ s. As a result of such speciation, we must consider equilibria of the type given in eqs 1 along with CV scan rates when interpreting CV data.

$$[(Zr_6BCl_{12})Cl_x(H_2O)_{6-x}]^{1-x} + Cl^- \rightleftharpoons [(Zr_6BCl_{12})Cl_{x+1}(H_2O)_{5-x}]^{-x} + H_2O \quad (1a)$$

$$+e^- \left\| -e^- \right. \qquad +e^- \left\| -e^- \right.$$

$$[(Zr_6BCl_{12})Cl_x(H_2O)_{6-x}]^{2-x} + Cl^- \rightleftharpoons [(Zr_6BCl_{12})Cl_{x+1}(H_2O)_{5-x}]^{1-x} + H_2O \quad (1b)$$

$Rb_5Zr_6Cl_{18}B$ dissolves readily in 12 M HCl to form a red solution. A cyclic voltammogram obtained with this solution exhibits a pattern that is quite similar to that shown in Figure 4a, but the half-wave potential ($E_{1/2}$) for 13/14 CBE couple shifts to −0.028 V (vs SHE) and the peak separation (ΔE_p) increases to 0.101 V. The peak ratio (i_p^c/i_p^a) is 0.97 when the scan rate is 5000 mV/s. When a slower scan (3000 mV/s) was used, the peak ratio decreased to 0.90. However, because Cl^-/H_2O exchange reactions occur over time scales shorter than a scan cycle, the i_p^c/i_p^a ratio cannot be viewed as a quantitative indicator of "chemical reversibility" of the redox reactions. Indeed, our isolation of **6** (an oxidized 13 CBE cluster compound) from an essentially identical solution indicates that the anodic reaction probably yields a stable 13 CBE species on the time scale longer than a CV scan. Since the equilibrium constants for reactions 1a,b are likely to be different and because the redox potentials for clusters will depend to some extent on the number of terminal chloride ligands, the observed values of ΔE_p can vary from "ideal" value 60 mV for reasons unrelated to the electrode reaction rate.

A cyclic voltammogram recorded for an HCl solution of $Na_4Zr_6Cl_{16}Be$ exhibits two distinct redox couples; the rest potential sits between these two couples at −0.421 V. On scanning of

the potential to more positive values, a one-electron oxidation wave that we assign to the 12/13 CBE redox couple is observed at $E_{1/2} = -0.275$ V (vs SHE) with a peak potential (ΔE_p) separation of 0.082 V and the peak ratio (i_p^c/i_p^a) of 0.69. When the potential is scanned in the negative direction past the rest potential, a one-electron reduction wave, assignable to 13/14 CBE redox couple, is observed at $E_{1/2} = -0.662$ V (vs SHE) with a peak potential separation (ΔE_p) of 0.083 V and the peak ratio (i_p^a/i_p^c) of 0.14. Compound **4** (with 13 CBEs), which was isolated from 12 M HCl, is one-electron oxidation product of the solid precursor, and as one would expect, the rest potential is bracketed by the 12/13 and 13/14 CBE redox couples. We again attribute the large value of peak potential separation ($\Delta E_p \approx 0.080$ V) to the spread in cluster speciation. The small value of peak ratio ($i_p^c/i_p^a = 0.69$) for the 12/13 CBE redox couple is probably due to the instability of the 12 CBE cluster species. The reduced peak ratio ($i_p^a/i_p^c = 0.14$) for the 13/14 CBE couple is more difficult to definitively rationalize. However, it is quite possible that the 14 CBE species serves as a catalyst for proton reduction and 13 CBE cluster is thereby regenerated at a rate comparable to the scan rate—after all, the 14 → 13 CBE oxidation occurs efficiently upon dissolution of the precursor solid in the first place. The large irreversible multielectron wave at positive potential (0.010 V) is attributed to cluster decomposition and formation of Zr^{IV} species.

Unfortunately, no well-defined redox couples are observed by cyclic voltammetry for the 12 M HCl solution containing C-centered clusters; the irreversible oxidative wave at 0.555 V undoubtedly signals cluster decomposition.

(d) Correlations in the Electrochemical Results. First, clusters with different interstitial atoms exhibit quite different cyclic voltammograms—scanning from the negative edge toward the positive edge of this CV "window". (The window ranges from −1.1 V where H^+ is reduced to H_2 to 1.1 V where Br^- is oxidized to Br_2 or 1.2 V where H_2O is oxidized to O_2.) Be-centered clusters all show two distinct redox waves for the 13/14 and 12/13 redox couples, besides a cluster decomposition wave. The potential difference ($\Delta E_{1/2}$) between 13/14 and 12/13 CBE couples is ∼0.4 V, which quite is comparable to the corresponding potential difference we observed in $AlCl_3$/ImCl ionic liquids. B-centered clusters (either chloride- or bromide-supported) display only the 13/14 redox couple (besides the decomposition wave) in their aqueous solution. No distinct one-electron redox waves (besides the oxidative decomposition wave) were observed for aqueous solutions containing C-centered clusters. Overall, the behavior we observe is similar to that seen in acidic molten salts.[47] These results clearly suggest that, if formed at all, $[Zr_6ZCl_{12}]^{3+}$ (Z = Be, B, C) clusters rapidly decompose to yield simple Zr^{IV} products in water or ionic liquids when the solvents are acidic.

The bromide-supported cluster species, $[Zr_6ZBr_{12}]^{n+}$, are weaker reducing agents than their chloride analogues, as evident from inspection of Table 5. If, for example, we compare the following electrochemical reactions on a glassy carbon electrode (potential vs SHE), we conclude that the chloride-supported cluster is apparently 0.099 V more easily oxidized than its bromide analogue:

$$[(Zr_6BCl_{12})(H_2O)_6]^+ + e^- \rightleftharpoons [(Zr_6BCl_{12})(H_2O)_6]^0 \qquad E_{1/2} = 0.060 \text{ V}$$

$$[(Zr_6BBr_{12})(H_2O)_6]^+ + e^- \rightleftharpoons [(Zr_6BBr_{12})(H_2O)_6]^0 \qquad E_{1/2} = 0.159 \text{ V}$$

Still, both the chloride- and bromide-supported clusters are oxidized at positive potentials in 4 M triflic acid and are too weakly reducing to reduce protons even in acidic solution.

We would expect that $[(Zr_6BCl_{12})(H_2O)_{6-x}Cl_x]^{1-x}$ anions formed by binding of chloride to the terminal positions on the cluster would more easily be oxidized than the hexaaquo species, $[(Zr_6BCl_{12})(H_2O)_6]^+$. Nevertheless, the observed shift in potentials on moving from 4 M triflic acid to 12 M HCl (from $E_{1/2} = 0.059$ V to $E_{1/2} = -0.028$ V) is quite modest, especially when we consider that no chloride ligands are bound in the first case and ∼4 are bound in the second case. This is in contrast to observations in CH_3CN and ionic liquids. In CH_3CN, the replacement of a single chloride ligand by CH_3CN gives rise to a potential shift of 0.19 V. ($[(Zr_6BCl_{12})(CH_3CN)Cl_5]^{4-/3-}$, $E_{1/2} = -0.98$ V; $[(Zr_6BCl_{12})Cl_6]^{5-/4-}$, $E_{1/2} = -1.17$ V; both vs 0.01 M $Ag/AgNO_3$ in CH_3CN.) On changing from the acidic $AlCl_3$/ImCl ionic liquid to the basic melt, wherein six chloride ligands are added to the cluster, a shift in the 13/14 CBE couple of 1.07 V is seen. ($(Zr_6BCl_{12})^{+/2+}$ in 60:40 $AlCl_3$/ImCl, $E_{1/2} = 0.70$ V; $[(Zr_6BCl_{12})Cl_6]^{5-/4-}$ in 40:60 $AlCl_3$/ImCl, $E_{1/2} = -0.365$ V; both vs Al/Al^{3+} in 60:40 $AlCl_3$/ImCl.)[47] Presumably, differences in the solvation of the clusters involving hydrogen bonding, dielectric constants, and coordinating ability are all involved in the profound differences we see in the very different range of redox potentials observed for the range of $[(Zr_6BCl_{12})(solv)_{6-x}Cl_x]^{1-x}$ species.

Conclusions

For the first time, the stability of reduced zirconium compounds in aqueous media has been demonstrated. The $[Zr_6BX_{12}]^+$ and $[Zr_6CX_{12}]^{2+}$ (X = Cl and Br) clusters exhibit sufficiently prolonged lifetimes in strongly acidic and/or halide-rich aqueous solutions that the pursuit of further coordination chemistry under these conditions is conceivable. Data obtained from CV studies in various aqueous solutions reveal that $[Zr_6BeX_{12}]^0$ (14 CBEs) and $[Zr_6BBr_{12}]^0$ (15 CBEs) clusters are good one-electron reducing agents and $[Zr_6BCl_{12}]^+$ and $[Zr_6BBr_{12}]^+$ clusters are, in practice, too weakly reducing to reduce protons, even in acidic solution. Cluster lifetimes are sufficiently long to enable crystallization of several cluster hydrates, whose structures segregate into two structure types that contain intriguing hydrogen-bonded networks within which $[(Zr_6ZCl_{12})X_6]^{m-}$ clusters are embedded.

Acknowledgment. We gratefully acknowledge the Robert A. Welch Foundation for its support through Grant A-1132 and the National Science Foundation for its support through Grant CHE-9623255. We extend our thanks to Dr. Richard Staples for collecting the single-crystal X-ray data set using a CCD-equipped X-ray diffractometer at Harvard University, purchased through NIH Grant 1S10RR11937-01. We also thank Professors D. J. Darensbourg and M. Y. Darensbourg for allowing us the use of their BAS electrochemical workstation.

Supporting Information Available: An X-ray crystallographic file in CIF format for the structure determinations of $[Rb_{0.44}(H_3O)_{4.56}][(Zr_6BCl_{12})Cl_6]\cdot 19.44H_2O$ (**3**), $(H_3O)_5[(Zr_6BeCl_{12})Cl_6]\cdot 19H_2O$ (**4**), $(H_3O)_5[(Zr_6MnCl_{12})Cl_6]\cdot 19H_2O$ (**5**), $(H_3O)_4[(Zr_6BCl_{12})Cl_6]\cdot 12.97H_2O$ (**6**), and $(H_3O)_4[(Zr_6BCl_{12})Br_6]\cdot 13.13H_2O$ (**7**). This material is available free charge via the Internet at http://pubs.acs.org.

IC9908423